



Selective purification of catecholates, hydroxamate and α -hydroxycarboxylate siderophores with titanium dioxide affinity chromatography

Philipp H. Egbers^a, Christian Zurhelle^a, Boris P. Koch^{b,c}, Alexandra Dürwald^d, Tilmann Harder^{a,b}, Jan Tebben^{b,*}

^a Faculty of Biology and Chemistry, University of Bremen, Leobener Str. 6, 28359 Bremen, Germany

^b Department of Ecological Chemistry, Alfred Wegener Institute, Helmholtz Centre for Polar and Marine Research, Am Handelshafen 12, 27570 Bremerhaven, Germany

^c University of Applied Sciences, An der Karlstadt 8, 27568 Bremerhaven, Germany

^d Pharmaceutical Biotechnology, Institute of Pharmacy, University of Greifswald, Felix-Hausdorff-Str. 3, 17487, Greifswald, Germany

ARTICLE INFO

Keywords:

Siderophores
Iron cycle
Metal oxide affinity chromatography
Ligand purification
Titanium dioxide

ABSTRACT

Siderophores, high affinity iron chelators, play a key role in the uptake of iron by microorganisms and regulate many biological functions. Siderophores are categorized by their chelating group, e.g., catecholates, hydroxamates, α -hydroxycarboxylates. Natural concentrations of siderophores are often either too low or sample matrices are too complex for direct analysis by, e.g., liquid chromatography – mass spectrometry. Therefore, both concentration and purification are prerequisite for reliable analyses. However, a chromatographic technique that is selective for all siderophore classes and affords high levels of purification is lacking. We developed a titanium dioxide affinity chromatography (TDAC) solid-phase extraction (SPE) that affords the selective purification of these siderophore classes from complex sample matrices with recoveries up to 82%. The one-step purification removed most non-ligand sample ‘contaminants’, therefore, affording the straightforward identification of siderophore peaks in base peak chromatograms. As a proof of concept, the bioinformatic processing, depepitation of known features and selection of significant features in the TDAC eluates afforded a fast identification of six novel siderophores (woodybactines) from bacterial supernatants. We propose TDAC SPE as a fast and cost-effective methodology to screen for known or discover novel siderophores in natural samples in combination with untargeted bioinformatic processing by, e.g., XCMS. The method is scalable and yielded large amounts of highly purified siderophores from bacterial culture supernatants, providing an effective quantitative sample clean-up for, e.g., NMR structure elucidation.

1. Introduction

Many bacteria, fungi and graminaceous plants produce organic ligands, termed siderophores, to scavenge the essential micronutrient iron (Fe). Siderophores are chemically diverse and considered ‘keystone metabolites’ that regulate various ecological roles ranging from niche adaptation to symbiosis and pathogenicity. The four most commonly occurring siderophores are classified into classes depending on their chelating group, namely catecholates, hydroxamates, α -hydroxycarboxylates and mixed ligand siderophores (Fig. 1, [1,2]). Natural

siderophore concentrations in the environment are notoriously low and sample matrices (e.g., soil extracts, pore water, seawater, microbial culture media) are often too complex for their direct instrumental analysis [3]. Therefore, both concentration and purification is prerequisite for reliable analyses. Reversed-phase or ion exchange chromatography is often used to concentrate and desalt samples, yet both methods show inconsistent recoveries across the polarity spectrum of siderophores and often result in siderophore fractions containing numerous other compounds in the same polarity spectrum. A selective purification of siderophores was first achieved with Immobilized Metal

Abbreviations: IMAC, Immobilized Metal Affinity Chromatography; DFOB, Desferrioxamine B; FOB, Ferrioxamine B; PB, Petrobactin; VB, Vibrioferrin; WBA, Woodybactin A; SPE, Solid phase extraction; ES, Elution solution; LC-HRMS, Liquid chromatography–high resolution mass spectrometry.

* Corresponding author.

E-mail address: jan.tebben@awi.de (J. Tebben).

<https://doi.org/10.1016/j.seppur.2022.122639>

Received 14 September 2022; Received in revised form 7 November 2022; Accepted 9 November 2022

Available online 14 November 2022

1383-5866/© 2022 The Authors. Published by Elsevier B.V. This is an open access article under the CC BY license (<http://creativecommons.org/licenses/by/4.0/>).

Affinity Chromatography (IMAC) based on the affinity of siderophores to free coordination sites of immobilized metal cations [4]. IMAC has been successfully applied to hydroxamate siderophores such as ferrioxamine and ferrichrome [5,6]. IMAC purification of the catechol bacillibactin only yielded a fragment with one catechol group while the intact siderophore with three catechol groups was not recovered [7]. Similarly, the mixed ligand siderophore pyoverdine could not be detected in IMAC eluates [6], suggesting that siderophores with high complex stability constants are not retained. Thus, a different type of affinity chromatography that enables concurrent analyses of siderophores independent of polarity and complex stability constant is highly desirable. Metal Oxide Affinity Chromatography (MOAC), particularly using titanium dioxide (TiO_2), can circumvent some of the issues of IMAC: Previous studies showed that catecholates and hydroxamates adsorb well on TiO_2 surfaces, therefore suggesting MOAC utilizing TiO_2 as a potential alternative for metal ligand extraction [8,9]. TiO_2 acts as an anion or cation exchanger depending on whether the surface hydroxyl groups are protonated or dissociated. Additionally, unsaturated Lewis acid sites on the surface exhibit ligand-exchange functionality [10]. We recently showed proof-of-concept that TiO_2 nanoparticle solid phase extraction (SPE) is well suited to extract and elute hydroxamate siderophores from complex matrices [11]. Hydroxamates form inner-sphere surface complexes on TiO_2 [12] and due to the unique conditions required to destabilize those complexes, hydroxamates can be largely separated from organic contaminants and inorganic salts. In contrast to outer-sphere surface complexes, whose formation is based on nonspecific interaction, like hydrogen bonding and electrostatic attraction (physisorption), inner-sphere surface complexes are not as susceptible to changes in solvent conditions [13]. Catecholates and α -hydroxycarboxylates are also known to form inner-sphere surface complexes with TiO_2 [14–18]. The elution of siderophores containing those functional groups from TiO_2 and, consequently, the application as chromatographic method is still unknown.

Here, we established a titanium dioxide affinity chromatography (TDAC) to concentrate and purify the three major siderophore classes, i. e., catecholates, α -hydroxycarboxylates and hydroxamates. The main aim was to concurrently analyze all siderophore types, yield high levels of purification and analyte recovery and to assess the scalability of this method. The project was divided into three objectives: (i) To develop and optimize a quantitative purification of four model siderophores with TiO_2 column chromatography, (ii) To achieve quantitative purification of siderophores from complex sample matrices, and (iii) To afford the discovery of novel siderophores with TDAC coupled with untargeted metabolomic profiling and bioinformatic data analysis.

2. Experimental

2.1. Materials and chemicals

All glassware and vessels were soaked in 10 % hydrochloric acid for at least 48 h and washed generously with ultrapure water prior to use. Reagents used for the preparation of the elution solutions, e.g., sodium dihydrogen phosphate monohydrate (e.g., NaH_2PO_4), and bacterial growth media (supporting information) were reagent grade (Roth, Sigma-Aldrich or VWR). Elution solutions were prepared by dissolving each salt in ultrapure water to $\frac{3}{4}$ of the final volume followed by pH adjustment with either 12 M hydrochloric acid or 10 M sodium hydroxide and then adjustment to the final volume. All anions tested were used with sodium as cation unless stated otherwise. Polypropylene solid phase extraction (SPE) cartridges (3 mL, 6 mL Chromabond) with fitting polyethylene filter elements were purchased from Macherey-Nagel. Desferrioxamine B (DFOB) was purchased as desferrioxamine mesylate (Sigma-Aldrich). Petrobactin (PB), vibrioferrin (VF) and woodybactin A (WBA) were prepared in our laboratories (supporting information: Siderophore Standard preparation). Titanium dioxide was obtained as oven clinker from rotary kilns (initial particle size > 1 mm, Kronos Worldwide, Inc., Nordenham Germany). The oven clinker was manually ground with mortar and pestle and wet sieved with nylon gauze filter units (50, 100 and 200 μm cut-off) until no turbidity of the wash water was recognizable. The 50 μm size fraction was collected and dried at 120 $^\circ\text{C}$ overnight and used for all SPE experiments. This TiO_2 had a surface area of 5.0 m^2/g (BET) and the D_{50} mass-median-diameter of 54.092 μm (Fig. S1). 200 or 500 mg of TiO_2 were weight in (± 5 mg) and filled into empty 3 or 6 mL SPE cartridges, respectively. To ensure reproducible extraction performances PE filter elements were used and the packed cartridges were compacted manually.

2.2. Instrumental

LC-HRMS analysis and all siderophore quantifications were performed with a Vanquish UPLC system coupled to a Q-Exactive Plus mass spectrometer, using a heated electrospray ionization source (both Thermo Fisher Scientific). The LC system was operated with a C18 column (C18 BEH, 100 \times 2 mm, 1.7 μm , equipped with guard-column, Waters) using the following settings: Solvent A = 0.1 % formic acid in ultrapure water, solvent B = 0.1 % formic acid in methanol; $T_{0 \text{ min}}$: B = 1 %, $T_{2 \text{ min}}$: B = 1 %, $T_{5.0 \text{ min}}$: B = 99 %, $T_{7.1 \text{ min}}$: B = 99 %, $T_{7.2 \text{ min}}$: B = 1 % with a flow rate of 0.35 mL min^{-1} . The effluent of the first 1.5 min was diverted to waste to limit salt deposits. The column oven was set to 32 $^\circ\text{C}$. The mass spectrometer was calibrated using Positive Ion Calibration

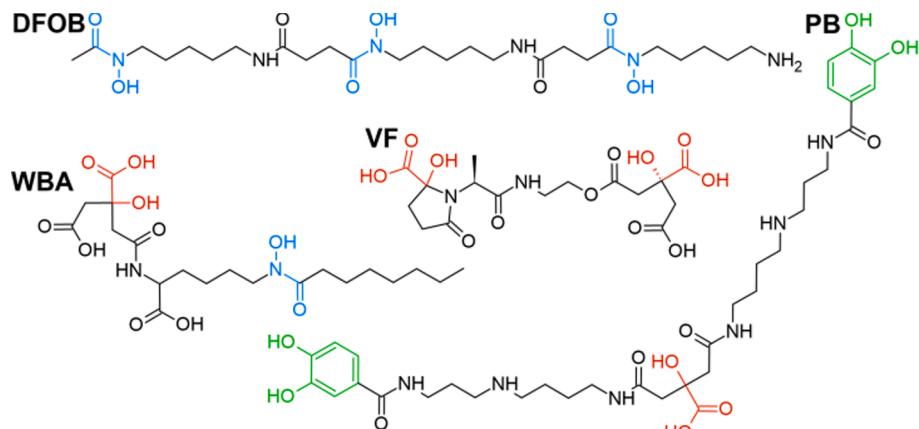


Fig. 1. Structures of four siderophores used in this study. (DFOB) desferrioxamine B, (WBA) woodybactin A, (VF) vibrioferrin and (PB) petrobactin. The three major functional groups hydroxamate (blue), catechol (green) and α -hydroxycarboxylate (red) are also highlighted. (For interpretation of the references to colour in this figure legend, the reader is referred to the web version of this article.)

Solution (Pierce, Thermo Fisher Scientific), all MS measurements were done in positive mode. All sample solutions were prepared in 1.5 mL short throat brown glass vials (Agilent Technologies). Data independent mode with a full scan resolution of 70,000 (m/z 200) followed by MS² experiments (normalized collision energy of 30, automatic gain control target of 3×10^6 and 50 ms maximum injection time) was used for the identification and quantification of siderophore standards. All siderophores were quantified using the exact mass ± 2.5 ppm of the precursor ions. I.e., DFOB was quantified using the sum of the DFOB ion ($[M + H]^+ C_{25}H_{49}N_6O_8$, calc. m/z 561.3606), the FOB ion ($[M + H]^+ C_{25}H_{46}N_6O_8Fe$, calc. m/z 614.2721) and the AFOB ($[M + H]^+ C_{25}H_{46}N_6O_8Al$, calc. m/z 585.3287) ion. VF was quantified using the sum of the apo-VF ($[M + H]^+ C_{16}H_{23}N_2O_{12}$, calc. m/z 435.1246) and the Fe-VF ($[M + H]^+ C_{16}H_{20}N_2O_{12}Fe$, calc. m/z 488.0360). WBA was quantified using the sum of the single charged apo-WBA ($[M + H]^+ C_{20}H_{35}N_2O_{10}$, calc. m/z 463.2286) and the Fe(III)-WBA ($[M + H]^+ C_{20}H_{32}N_2O_{10}Fe$, calc. m/z 516.1401). PB was quantified as the sum of the single ($[M + H]^+ C_{34}H_{51}N_6O_{11}$, calc. m/z 719.3610) or double protonated apo-PB ($[M + 2H]^{2+} C_{34}H_{52}N_6O_{11}$, calc. m/z 360.1842). The corresponding calibration curves, chromatograms and mass spectra are listed in the supporting information (Fig. S4, S5, S6, S8). Each siderophore was confirmed by MS/MS fragmentation (Fig. S7) in comparison to literature spectra. NMR experiments were performed in 1.7 mm microtubes at 300 K with deuterated water (D₂O) or dimethyl sulfoxide (DMSO-*d*₆) and at 292 K with deuterated methanol (MeOD) using an AVANCE II 600 MHz NMR spectrometer a CPTCI microcryoprobe (Bruker). Bruker standard pulse programs were used.

2.3. Bacterial cultures

The marine bacteria *Marinobacter* sp. DG870 was originally isolated from dinoflagellate *Gymnodinium catenatum* [19] and used to purify vibrioferrin (VF). *Paracoccus* sp. AR04 was originally isolated during the Antarctic RV Polarstern cruise PS124 [20] and used to purify petrobactin (PB). *Marinomonas* sp. LOF59-2 was originally isolated from a bloom of the haptophyte *Chrysochromulina leadbeateri* in northern Norway during RV Heincke expedition HE533 [21,22] and used for the purification of woodybactin A (WBA). All strains were cultivated at 18 °C in Fe-deficient bacterial growth medium (supporting information), prepared with Chelex 100 (Bio-Rad, USA) using the column method described by the manufacturer. 1 L of autoclaved growth medium was filled into acid-washed and sterilized 2-L flasks and inoculated with bacteria ($n = 3$ per bacterium). The production of siderophores was monitored regularly with the CAS assay [23].

2.4. Siderophore standard preparation

CAS-active bacterial cultures were centrifuged (14000 rpm) and the supernatants concentrated on a column packed with polystyrene/divinylbenzene resin (Diaion HP20), desalted with ultrapure water and then eluted with methanol. The methanol eluate was then dried under vacuum. The crude extracts were dissolved in minimal amounts of ultrapure water and fractionated by time on a C18 semipreparative HPLC. CAS-active fractions were pooled and concentrated under vacuum. Aliquots of purified and dried extracts were dissolved in deuterated DMSO-*d*₆ (WBA), MeOD (PB), or D₂O (VF), respectively. Each solvent contained an internal standard, namely tetramethylsilane (conc. $7.36 \times 10^{-2} \text{ mol} \times \text{L}^{-1}$) in DMSO-*d*₆, dioxane (conc. $1.17 \times 10^{-2} \text{ mol} \times \text{L}^{-1}$) in MeOD, and dimethyl sulfoxide (conc. $1.88 \times 10^{-3} \text{ mol} \times \text{L}^{-1}$) in D₂O, respectively. Peak integration and quantification were done by multiplet analysis in MestreNova 11.0. Woodybactin B (Fig. S8) was quantified with the integrals of C-7 (4.14 ppm, q, $J = 8.0$ Hz, 1H), C-14 (2.33 ppm, t, $J = 7.8$ Hz, 1H) and C-20 (0.86 ppm, t, $J = 6.8$ Hz, 3H). Petrobactin (Fig. S7) was quantified with the integrals of C-4/C-5 (6.92 – 6.78 ppm, 4H), C-11 (2.97 ppm d, $J = 8.7$ Hz, 4H), C-16 (2.78 – 2.51 ppm, 4H) and C-13 (1.75 ppm, s, 4H). Vibrioferrin (Fig. S9) was quantified using the

integrals of C-3' (1.47 ppm, d, $J = 7.2$ Hz, 3H). The presence of each siderophore in the purified fractions was confirmed by MS² experiments (Fig. S8).

2.5. TDAC preparation

3 mL SPE cartridges (Chromabond, Macherey-Nagel) were packed with 200 mg of TiO₂. Our earlier study showed that the adsorption capacity of TiO₂ was orders of magnitude higher than any expected analyte concentration (e.g., for DFOB $15.7 \pm 0.2 \mu\text{mol mg}^{-1} \text{TiO}_2$) [11]. Columns were conditioned prior to use with 6 mL of 0.25 M NaH₂PO₄ at pH 2.4, followed by 6 mL of ultrapure water, 6 mL of 20 mM NaOH and 18 mL of ultrapure water. Siderophore adsorption was then performed from 2 mL samples containing either 10 μM of one or 10 μM of all four model siderophores (DFOB, VF, PB and WBA in 0.5 M NaCl, pH 4, 99 % adsorption efficiency). The flow rate was adjusted to one drop per second. Subsequently, SPE cartridges were washed with 6 mL of ultrapure water before elution with 2×1 mL of elution solution (ESs 1–32) or organic solvents (acetonitrile, acetone or methanol). TDAC columns can be regenerated (supporting information: TDAC protocol).

2.6. Siderophore quantification

To avoid matrix or ionization effects caused by the different elution solution compositions (Fig. S4, S6), counter solutions (Table S2) were used to unify the matrix of all eluates prior to analysis (Fig. S6). 50 μL of the elution solution was diluted with 450 μL of the corresponding counter solution directly after TDAC elution. ¹³C-labelled phenylalanine and hydroxybenzoic acid were added to monitor peak intensities over all injections (Fig. S5). All experiments were conducted at pH 4 since pre-experiments showed that the adsorption of the α -hydroxycarboxylate siderophore (VF) onto TiO₂ is favoured at weakly acidic conditions, whereas the hydroxamate (DFOB), catecholates (PB) and mixed ligand (WBA) showed no such distinct pH dependence (Fig. S2). Each experiment was performed in triplicates. The adsorption efficiencies (calculated as amount of analyte detected in the SPE permeate in comparison to the original sample) for all tested siderophores were higher than 93 % for all treatments and replicates prior to elution. Desorption efficiencies (%) were determined relative to the amount of adsorbed analyte.

2.7. Elution profiles

The elution profile of a sample containing multiple siderophore classes was tested using a 2 mL of a siderophore mixture containing 10 μM DFOB, PB, VF and WBA in 0.5 M NaCl at pH 4. This sample was passed over TDAC SPE cartridges (200 mg, 3 mL). Cartridges were rinsed with 12 mL of ultrapure water before elution with ES7 (0.1 M NaH₂PO₄, pH 2.4), ES14 (0.1 M Na₂SO₄, pH 12.6), ES15 (5.6 M NH₃, pH 12.6) or ES17 (1 mM NaH₂PO₄, pH 2.4). The choice of selected elution solutions used in this experiment is based on the results of the elution solution optimization experiment (Table 1). 8×1.0 mL fractions were collected and elution solutions were diluted with the corresponding counter solution directly after elution.

2.8. Siderophore purification from bacterial culture media

50 mL of cell-free and CAS negative bacterial culture supernatant was adjusted to pH 4 using hydrochloric acid (32 %) and spiked with DFOB (3.75 μM final concentration), PB, VF and WBA (75 μM final concentration each). We chose a bacterial culture supernatant as complex sample matrices because these contain a mixture of highly concentrated and chemically diverse compounds that often interfere with chromatographic purification and detection (e.g., salts, polysaccharides, lipids, proteins). The 6 mL, 500 mg TiO₂ SPE cartridge was conditioned as described above and the sample was applied at a flow rate of less than one drop per second. The column permeate (~50 mL)

Table 1

Desorption efficiencies of Desferrioxamine B, Vibrioferrin, Petrobactin and Woodybactin A in % from 3 mL, 200 mg TDAC depending on elution solution composition.

Elution solution and composition	DFOB		VF		PB		WBA	
	Single	Mix	Single	Mix	Single	Mix	Single	Mix
ES1 5 M NaH ₂ PO ₄ , pH 2.4	29.3±3.9	25.3±1.6	56.5±5.2	35.3±1.5	69.3±2.5	45.6±8.6	3.2±0.5	ND
ES2 5 M NaCl, pH 2.4	1.7±0.4	2.6±0.6	ND	ND	ND	ND	ND	1.2±0.8
ES3 0.5 M NaH ₂ PO ₄ , pH 2.4	30.4±1.6	28.9±2.2	58.2±4.4	49.2±1.8	30.2±3.5	23.3±7.4	18.2±8	12.8±1.5
ES4 0.5 M NaCl, pH 2.4	2.0±0.2	3.9±1.2	ND	ND	1.2±0.4	ND	ND	1.5±0.5
ES5 0.5 M Na ₂ SO ₄ , pH 2.4	7.5±0.2	9.9±1.4	20.3±1.7	10.8±1.0	1.3±0.1	2.7±1.9	ND	1.8±0.6
ES6 0.5 M NaH ₂ PO ₄ /CaCl ₂ , pH 2.4	13.1±0.7	14.0±2.0	20.3±2.3	19.2±2.4	23.1±1.1	14.8±1.9	17.3±9.1	12.9±3.1
ES7 0.1 M NaH ₂ PO ₄ , pH 2.4	18.5±1.5	20.7±2.1	49.4±1.3	29.8±1.9	6.8±2.4	3.5±1.2	20.8±6.4	7.6±2.1
ES8 0.1 M NaCl, pH 2.4	1.0±0.2	1.2±0.2	ND	2.5±0.3	1.3±0.4	ND	ND	ND
ES9 0.1 M Na ₂ SO ₄ , pH 2.4	3.6±1.0	5.1±0.5	3.5±0.7	3.5	1.1±0.4	ND	ND	ND
ES10 Citric acid 20%	21.4±5.8	19.5±4.0	21.8±3.2	2.7	18.8±1.5	15.4±2.2	16.9±3.3	8.1±3.8
ES11 0.5 M NaH ₂ PO ₄ , pH 7	30.5±2.7	29.4±3.9	24.5±6.8	22.5	2.9±1.2	3.5±1.4	20.9±4.2	16.8±4.7
ES12 0.1 M NaH ₂ PO ₄ , pH 12.6	79.9±1.7	82.4±5.5	ND	ND	43.3±0.2	31.6±7.8	78.7±11.1	68.4±5
ES13 0.1 M NaCl, pH 12.6	68.6±1.8	68±0.4	5.7±2.5	10.7	32.1±0.4	20.2±6.2	59.1±9.2	49.4±3.4
ES14 0.1 M Na ₂ SO ₄ , pH 12.6	73.9±1.8	73.8±2.4	ND	ND	22.5±0.4	19.1±4.1	71.6±7.7	66.3±4.6
ES15 5.6 M NH ₃ , pH 12.6	39.1±1.2	37.4±2.9	ND	ND	73.1±6.1	69.6±11.4	32.6±4.4	11.9±5.8

ND = not detected, DFOB = Desferrioxamine B, VF = Vibrioferrin, PB = Petrobactin, WBA = Woodybactin A.

More intense green coloration shows better desorption efficiency.

was collected and directly measured by LC-HRMS. The column was washed with 12 mL of ultrapure water, 6 mL of methanol and again 12 mL of ultrapure water. The column was eluted with 2 mL elution solution (ES3: 0.5 M NaH₂PO₄, pH 2.4). The added solution was kept on the column overnight to achieve maximum desorption (10 h). The eluate was measured via LC-HRMS without any further steps. Siderophore quantification was achieved via external calibration in the corresponding elution solution.

2.9. Untargeted siderophore screening

To screen for siderophores, 3 mL of pH adjusted (pH 4) and cell-free bacteria culture supernatant (*Pseudoalteromonas* sp. LOF198-2, *Marinomonas* sp. LOF59-2) were extracted with TiO₂ SPE cartridges (200 mg, 3 mL). The supernatant of culture LOF198-2 showed strong CAS activity whereas the supernatant of LOF59-2 showed no CAS activity. Columns were prepared similarly to the experiments described above. The first milliliter of permeate was collected and cartridges were washed with 6 mL ultrapure water, 6 mL 0.5 M NaCl pH 4 and eluted with either 1.5 mL of ES3 (0.5 M NaH₂PO₄, pH 2.4) or (ES14 0.1 M Na₂SO₄, pH 12.6). The alkaline elution solutions were neutralized with hydrochloric acid (12 M) directly after extraction. Medium blanks were processed the same way. All samples were prepared in triplicates. 1 µL aliquot of each sample was analyzed by LC-HRMS as described above. LC-HRMS data were exported to mzXML using msconvert, and processed with XCMS using standard parameters (UPLC/Q-Exactive #3110) [24]. The list of significant features generated by XCMS was used to generate an inclusion list for the data independent acquisition of MS² spectra with a retention time window of ± 15 sec, an isolation window of ± 0.75 m/z and a normalized collision energy of 30.

3. Results and discussion

3.1. Optimal elution strategy of TDAC

The elution of strongly adsorbing siderophores, such as

hydroxamates, from TiO₂ is only achieved by simultaneous adjustment of the elution solution pH and ionic strength [11]. To determine optimal desorption conditions of α-hydroxycarboxylate, hydroxamate and catecholate siderophores from TiO₂, 15 different elution conditions were evaluated for each siderophore class (Table 1). Further, we then investigated if the presence of multiple siderophore classes in the same sample alter the elution behaviour. We also determined if co-adsorbed siderophores can be sequentially eluted, testing 32 elution solutions (Table 1, Table S3).

The best desorption efficiency of the hydroxamate siderophore DFOB were achieved with the alkaline ESs 12–14, containing 0.1 M phosphate, chloride or sulphate at pH 12.6 (up to 79.9 ± 1.7 %, Table 1). It was also shown that other adsorbed siderophores did not change the elution behavior of DFOB from TiO₂, resulting in desorption efficiencies of up to 82.4 ± 5.5 %. The observed elution behavior of DFOB was in accordance with the optimized elution conditions of DFOB from TiO₂ nanoparticles [11]. ES15 (NH₃, pH 12.6) showed poorer desorption efficiencies for the single DFOB sample (39.1 ± 1.2 %) as well as for the siderophore mix sample (37.4 ± 2.9 %) compared to the ESs 12–14, emphasizing that DFOB desorption required higher ionic strength. The anions used in the alkaline elution solution had almost no impact on the observed desorption efficiencies whereas under acidic conditions the presence of chloride and sulfate resulted in negligible elution of adsorbed DFOB. Only the addition of citrate and phosphate increased elution of DFOB under acidic conditions. Phosphate is the hardest Lewis base among the tested anions and may therefore compete most with adsorbed siderophores for Lewis acid binding sites on the TiO₂. This is supported by literature demonstrating that phosphate anions form strong bidentate inner-sphere surface complexes under acidic conditions with different metal oxide surfaces [25]. Surprisingly, increased phosphate concentrations in ES1 (5 M NaH₂PO₄, pH 2.4) did not lead to higher desorption efficiencies of adsorbed DFOB (29.3 ± 3.9 %) than ES3 (28.9 ± 2.2 %), containing only a tenth of the phosphate compared to ES1. Whereas ES3 showed better desorption efficiency than ES7 (0.1 M NaH₂PO₄, pH 2.4) (20.7 ± 2.1 %). This may be explained with phosphate being a kosmotrope, therefore the elution solution viscosity increases with phosphate

concentration [11]. We interpret the lower desorption efficiencies at near-saturated phosphate concentrations as a consequence of increased viscosity and the resulting poorer exchange between stationary and liquid phases. The addition of Ca^{2+} (ES6, 0.5 M $\text{NaH}_2\text{PO}_4/\text{CaCl}_2$, pH 2.4) did not alter the desorption of DFOB from TiO_2 in contrast to the desorption of DFOB from natural soil samples [26]. This result underlined that the positively charged terminal amine group was not involved in the DFOB TiO_2 interaction.

The best desorption efficiencies of the α -hydroxycarboxylate siderophore VF in the single siderophore experiment was obtained with the acidic phosphate eluents ES1 ($56.5 \pm 5.2\%$), ES3 ($58.2 \pm 4.4\%$) and ES7 ($49.4 \pm 1.3\%$). Surprisingly, the use of citric acid (ES10) as a competing agent did not result in increased displacement of VF ($21.8 \pm 3.2\%$) compared to phosphate, although it was expected that the α -hydroxycarboxylate groups of VF should be labile to substitution with the same functional group if present in high concentrations. Besides citric acid, the addition of sulfate under acidic conditions resulted in a similar desorption efficiency of VF ($20.3 \pm 1.7\%$). Only chloride did not enhance the elution VF. This may be explained with the fact that sulphate ions form mono- or bidentate inner-sphere surface complexes with TiO_2 under acidic conditions similar to phosphate, whereas chloride anions are likely to form only monodentate inner-spherical or weaker outer-spherical complexes. Comparing the results of the single siderophore experiment with the data of the siderophore-mix experiment, the interpretation is that co-adsorbed siderophores affect the desorption behavior of VF. In general, the observed desorption efficiencies are reduced, especially in case of the citrate containing elution solution ES10 (down to $2.7 \pm 0.4\%$). This difference highlights that further studies are needed to understand what effects are involved in the desorption of VF from TiO_2 .

The best desorption of the catechol-type siderophore PB in the single siderophore as well as in the siderophore-mix experiment was achieved with the alkaline ammonia solution ES15 ($73.1 \pm 6.1\%$ and $69.6 \pm 11.4\%$, respectively). These findings did not fit the expectations since catecholates are labile to oxidation under alkaline conditions [27]. The second best desorption efficiencies ($69.3 \pm 2.5\%$ and $45.6 \pm 8.6\%$, respectively) were observed for the acidic phosphate solution ES1 (5 M NaH_2PO_4 , pH 2.4). In comparison to the other siderophores, it is noticeable that only in the case of PB better desorption efficiencies were observed for ES1 than for ES3 or ES7. However, this confirmed previous findings of catechol desorption from TiO_2 under acidic conditions [28–30]. ES10 (citric acid 20%), previously tested for flavonoid desorption from TiO_2 [28], resulted only in a desorption efficiency of $<20\%$, similar to the observed desorption efficiencies for the other siderophores. As expected, ES5 (0.5 M Na_2SO_4 , pH 2.4) did not increase the desorption of PB ($<5\%$), because sulphate anions show lower affinities for TiO_2 than catecholates under acidic conditions [16]. PB desorption efficiencies with ES1, ES3, ES4 (0.5 M NaCl , pH 2.4), ES7 and ES11 (0.5 M NaH_2PO_4 , pH 7) supported the effect of phosphate concentration and pH on catechol desorption from TiO_2 : A low pH alone (ES4, $<2\%$) as well as phosphate at neutral conditions did not recover PB (ES11, $<5\%$), while the combination of both factors with increasing phosphate concentrations leads to increased desorption efficiencies. Contrary to our expectations, PB was detected in all alkaline elution solutions even with the highest desorption efficiency observed for ES15. Gulley-Stahl et al. showed that the catechol surface complex formed on TiO_2 depends on the pH during adsorption [13]. Acidic conditions (pH 3) led to the binding via two hydrogen bonds or to the monodentate binding, whereas neutral-alkaline conditions lead to mono- or binuclear bidentate binding [13]. Because the bidentate complexation exhibits higher binding strength to the TiO_2 surface [31] these findings suggest that at pH 4, PB forms mono- and bidentate catecholate TiO_2 complexes simultaneously, possibly leading to different conditions necessary for their desorption. This in turn may be the reason for PB detected in the acidic phosphate and the alkaline solutions. Why the composition of the alkaline solutions had an effect on the desorption efficiency of PB needs further investigation.

The best desorption efficiencies of the mixed hydroxamate- α -hydroxycarboxylate siderophore WBA was achieved with alkaline elution solutions ES12 and ES14 ($>70\%$). The desorption behaviour and observed efficiencies of WBA were similar to the hydroxamate-type DFOB but differed from the α -hydroxycarboxylate-type VF. This observation suggests that the hydroxamate group in WBA (Fig. 1) had a greater influence on the interaction with the TiO_2 surface than the α -hydroxycarboxylate group. The composition of the alkaline solutions (ESs 12–15) changed the elution of WBA in contrast to DFOB. Although phosphate, sulphate and chloride have no affinity to TiO_2 under alkaline conditions due to electrostatic repulsion [25,32,33], we observed increased elution of the mixed-type siderophore WBA with alkaline phosphate and sulphate solutions. This result may be attributed to differences in the ionic strength and Lewis base hardness of the ions and requires further investigation. WBA showed the worst desorption efficiencies for the acidic phosphate solutions compared to the three different model siderophores raising the question if the desorption of WBA is rendered by increasing viscosity.

3.2. Elution profiles of siderophores from TiO_2

We tested if the different elution behaviour of hydroxamates, catecholates and α -hydroxycarboxylates from TiO_2 allowed the selective purification of a sample with multiple siderophore types. For the selective purification of the four different siderophores, the elution solutions ES7, ES14, ES15 and ES17 (Table S3) were investigated. These four solutions were chosen because the desorption efficiencies for the siderophore-mix experiment (Table 1) suggested that these elution solutions could lead to the enrichment of one of the siderophores at a time. The elution profile obtained for ES7 (Fig. 2A) displays that under these conditions (0.1 M NaH_2PO_4 , pH 2.4) VF and DFOB show a similar elution behaviour, with the majority of the desorbed siderophore detected in the second millilitre of eluate. The overall desorption efficiency for VF and DFOB were determined as 47.2% and 42.2% , respectively. However, particularly remarkable about this profile is the elution behaviour of PB. The desorption efficiency of ES7 was not considered to be particularly high for PB, as only a desorption efficiency of $3.5 \pm 1.2\%$ was detected at an elution volume of 2 mL. It appears that by quadrupling the volume, the desorption efficiency was increased up to 81.1% . In contrast to the other siderophores, the eluted PB was not concentrated at an elution volume of 2 mL but at 4 mL. In contrast, the desorption efficiency for WBA could not be increased by increasing the volume. Using ES17 (1 mM NaH_2PO_4 , pH 2.4, Table S3) as the elution solution led to a drastic change in the elution profiles compared to ES7 (Fig. 2B). The decreased phosphate concentration caused the collapse of DFOB and PB desorption efficiencies (2.2% and 1.4% , respectively), whereas the desorption efficiency of VF remained above 34% . WBA also did not show such distinct changes in desorption efficiency. The elution profiles obtained for ES14 show a more rapid elution of DFOB and PB compared to the ones observed for ES7 (Fig. 2C). Especially, in case of DFOB, roughly 75% of the eluted siderophore (summed desorption efficiency 82%) was detected in the first fraction. The highest desorption efficiency for ES14 was detected for WBA with 97.7% . WBA showed a less distinct elution profile than DFOB. VF, on the other hand, was not detected in any of the eight fractions, which is consistent with the results in Table 1. Despite the same pH value, the elution profiles of ES14 and ES15 differ considerably (Fig. 2D). DFOB and WBA showed a broader elution profile whereas the elution of PB was enhanced, resulting in 80.2% desorption efficiency with the majority of eluted PB detected in the first fraction. Similar to the results for ES14, VF was also not detected in any of the elution fractions of ES15.

Our results suggest that a single-step elution with acidic phosphate solution (>0.1 M phosphate) is most suited for the untargeted concurrent screening of all siderophore classes. If, on the other hand, a specific siderophore class is targeted, the elution profiles obtained recommend tailoring the extraction protocol to the composition of the sample.

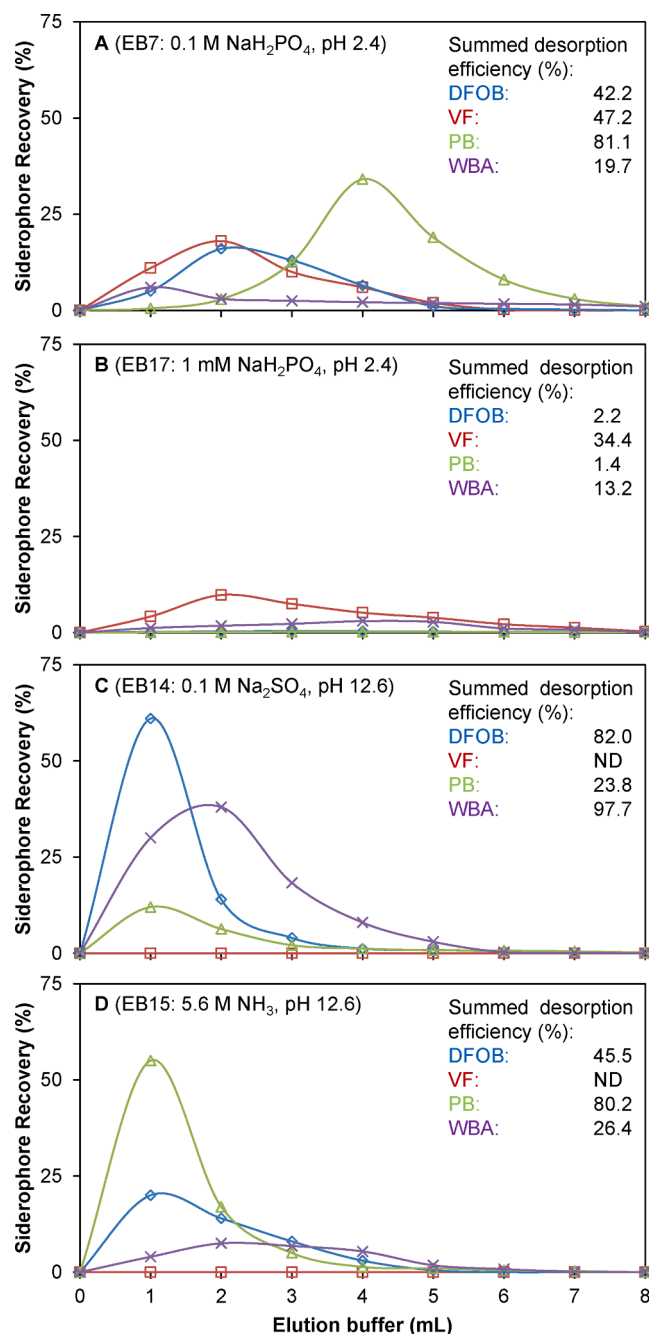


Fig. 2. Elution profiles of an equimolar solution (10 μ M) of DFOB (blue diamonds), VF (red squares), PB (green triangles) and WBA (purple crosses) in 2 mL of 0.5 M NaCl (pH 4), using a 3 mL, 200 mg TiO₂ column in 1 mL fractions. Columns were washed with 12 mL ultrapure water before elution. Elution was conducted with four different elution solutions (A-D). The summed recoveries are the summed percentages of eluted fractions 1–9 for each of the four model siderophores. (For interpretation of the references to colour in this figure legend, the reader is referred to the web version of this article.)

3.3. Siderophore extraction from complex sample matrices

The performance of TDAC for purification of siderophores from complex sample matrices was tested using a bacterial culture supernatant spiked with four model siderophores DFOB, VF, PB, and WBA. The total recoveries were determined as 62 %, 45 %, 82 % and 25 % respectively. These recoveries were similar to the summed desorption efficiencies found for standards extracted without organic background using 8 mL of the less concentrated phosphate solution ES7 for elution

(Fig. 2A). Therefore, TDAC is robust against high concentrations of organic and inorganic contaminants present in bacterial growth media which typically contain a plethora of possible co-eluting and interfering compounds. The chromatograms and mass spectra of the crude bacterial culture supernatant sample and the TDAC eluate, confirmed the high specificity of TDAC for siderophore purification from complex sample matrix (Fig. 3). The background-subtracted base peak chromatograms of the crude bacterial culture supernatant sample showed more peaks (Fig. 3, A) in comparison to the base peak chromatogram of the TiO₂ eluate in which the peaks of the siderophores were the dominating features (Fig. 3, B). This result was also reflected by the spectra extracted at the retention times of the siderophores: The siderophore ions were only minor ions in the spectra obtained from the complex sample (Fig. 3, A1–A5).

No **vibrioferri**n peak, for example, was discernible in the base peak chromatogram of the complex sample (Fig. 3, A retention-window 1, red), while a peak was easily recognized in the TDAC eluate (Fig. 3, B). The averaged mass spectrum for the same retention time showed the siderophore ion as the dominating signal for the TDAC eluate (Fig. 4, B1; apo-VF, $[M + H]^+ C_{16}H_{23}N_2O_{12}$, calc. m/z 435.1246) in comparison to the spectra of the raw bacterial supernatant (Fig. 3, A1) that were dominated by contaminants. The same was true for the other tested siderophores **petrobactin** (Fig. 3, retention window 2, green), **ferrioxamine** (Fig. 3, retention window 3 and 4, blue) and **woodybactin** (Fig. 3, retention window 5, purple). The doubly charged apo-PB ($[M + 2H]^{2+} C_{34}H_{52}N_6O_{11}$, calc. m/z 360.1842) was the dominant peak in the averaged mass spectrum of retention-time 3 for the TDAC purified sample (Fig. 3, B2). DFOB ($[M + H]^+ C_{25}H_{49}N_6O_8$, calc. m/z 561.3606) as well as the corresponding Fe(III)-complex FOB ($[M + H]^+ C_{25}H_{46}N_6O_8Fe$, calc. m/z 614.2721) were also the dominant peaks in the TDAC sample (Fig. 4, B3 and B4) but not in the crude supernatant (Fig. 3, A3 and A4). apo-WBA ($[M + H]^+ C_{20}H_{35}N_2O_{10}$, calc. m/z 463.2286) had a relative intensity of < 25 % in the crude sample (Fig. 4, A5) but was the highest peak in the TDAC eluate (Fig. 3, B5). The asterisked peak at 5.92 min was attributed to WBA-H₂O ($[M + H]^+ C_{20}H_{33}N_2O_9$, calc. m/z 445.2181).

This peak was also detected in the original WBA standard without TDAC treatment. In summary, the data suggests that all siderophores were recovered from a crude bacterial supernatant by the TDAC method with an observable clean-up of both the chromatogram as well as averaged mass spectra (Fig. 3, A vs B). In comparison to the crude sample, all siderophores could be identified in the LC-HRMS base peak chromatograms. LC-HRMS was used for all analyses here, however, siderophore detection and quantification is likely also possible with lower resolution mass spectrometers after TDAC SPE clean-up as suggested by the rather large mass range used for generating the extracted ion chromatograms (± 5 ppm).

3.4. Untargeted siderophore screening

Untargeted LC-HRMS data were recorded and analyzed for two siderophore producing strains each analyzed with and without TDAC pre-treatment. The untargeted analysis of the data (XCMS [24]) showed a clear reduction of the sample complexity after TDAC purification. For strain CLOF198-2, for example, 15,462 peaks were detected in the untreated bacterial supernatant in comparison to 3574 in the TDAC treated sample. For the LOF59-2 strain 15,314 peaks were detected in the crude and 3250 in the TDAC sample. A large proportion of these peaks were removed by subtraction of peaks also found in procedural blanks. All siderophores produced by the CLOF198-2 strain could be easily identified as significant features in comparison to the procedural medium TDAC control (DFOG1: $p \leq 0.005$; FOG1: $p \leq 0.008$). The analysis of the LOF59-2 TDAC sample in comparison to the procedural control also identified the WBA peak as a significant feature ($p < 0.005$) as well as further candidates with $p < 0.005$. Based on the feature list generated by the untargeted method, we generated an inclusion list for the targeted

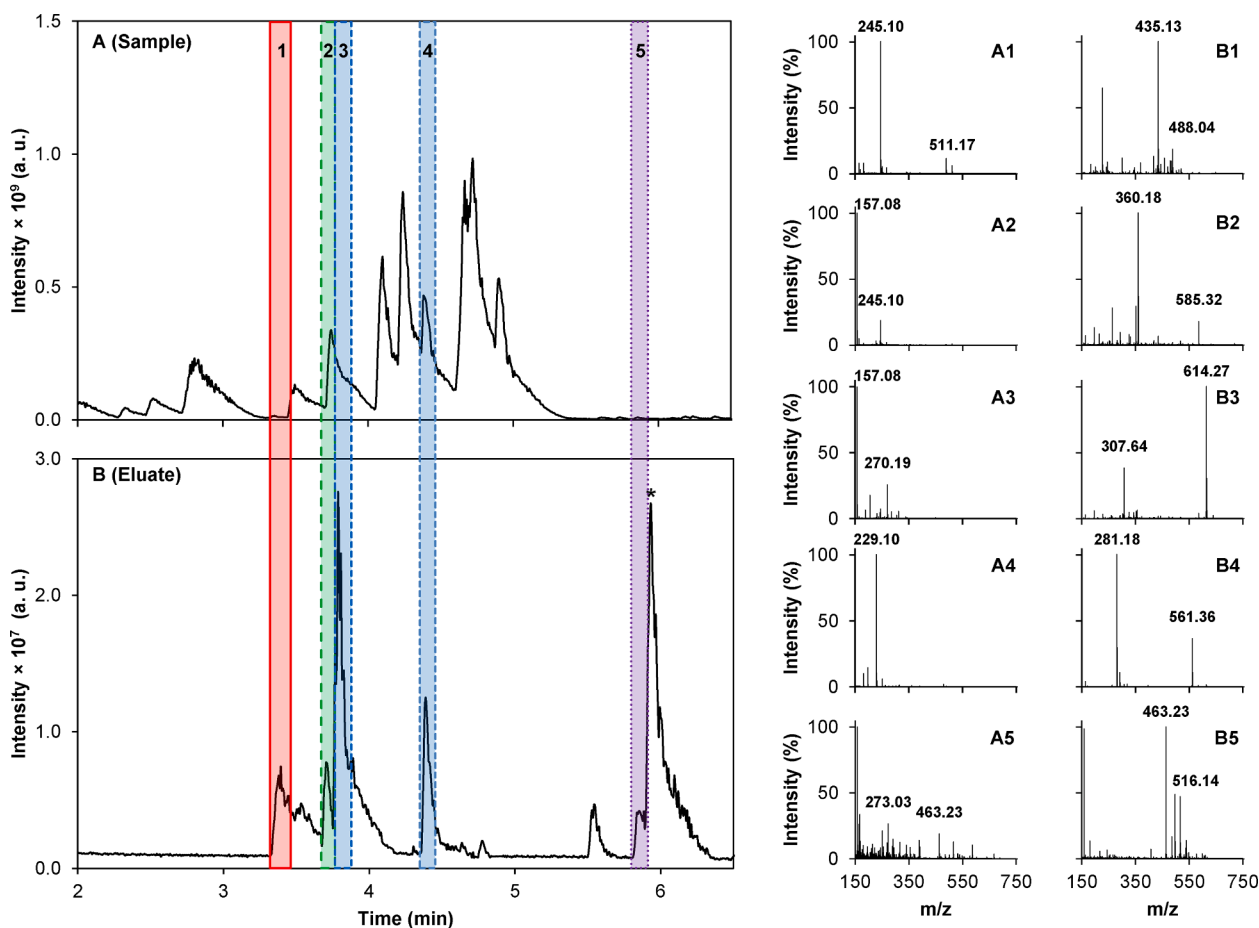


Fig. 3. Background-subtracted base peak chromatograms (LC-ESI(+)-HRMS) of a bacterial culture supernatant spiked with DFOB, VF, PB and WBA (final concentration of 3.75, 75, 75 and 75 μM , respectively) **A:** without processing (crude sample) and **B** after TDAC (0.5 M NaH_2PO_4 , pH 2.4) purification. The colored areas mark the time retention-time windows for 1, red: vibrioferrin; 2, green: petrobactin; 3, blue: ferrioxamine; 4, blue: ferrioxamine; 5, purple: woodybactin used to average the mass spectra of the same retention-time for the unprocessed bacterial supernatant (A1-A5) and TDAC purified sample (B1-B5). (For interpretation of the references to colour in this figure legend, the reader is referred to the web version of this article.)

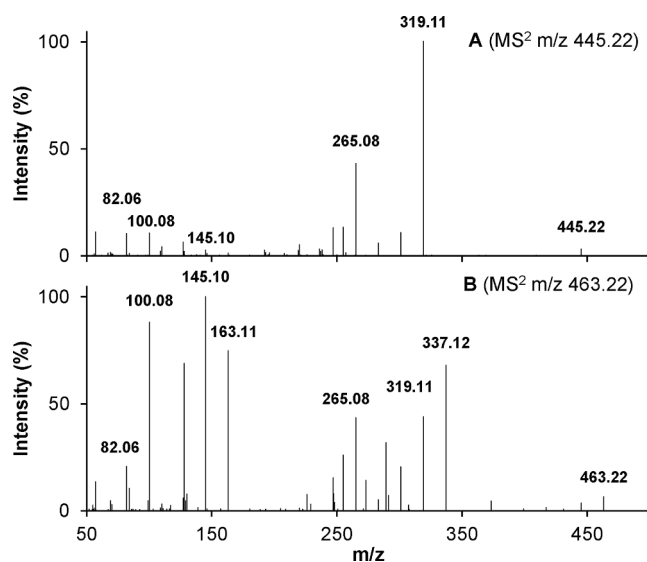


Fig. 4. (A) MS^2 spectra of $[\text{M} + \text{H}]^+$ m/z 445.22 corresponding to the marked peak (*) at 5.92 min in Fig. 3.C. (B) MS^2 spectra of $[\text{M} + \text{H}]^+$ m/z 463.22 corresponding to WBA (Peak 5) at 5.87 min.

fragmentation of significant features. This approach identified six known and six novel woodybactin derivatives in the TDAC eluate using typical daughter ions for identification (Table S4, Fig. S13). The reduction of sample complexity as well as the straight forward dereliction and subsequent identification of novel siderophores from the list of significant features highlights the potential of TDAC for siderophore discovery.

4. Conclusion

In this study, we developed a titanium dioxide affinity chromatography (TDAC) for the selective purification of three main siderophore classes, i.e., catecholates, α -hydroxycarboxylates, hydroxamates and mixed ligands. TDAC is scalable and selectively purified siderophores and almost completely removed organic 'contaminants' from a bacterial culture supernatant mix containing all four types of model siderophores with recoveries of up to 82 % (PB). Thus, the TDAC SPE method simplifies the purification of siderophores and may facilitate the discovery and quantification of siderophores in a variety of natural matrices such as seawater, soil or medical samples. While TDAC is likely sufficient for many research applications, a major methodological challenge will be to achieve the same recovery and selectivity for pM concentrations of siderophores in natural samples. For this application, co-adsorption, self-assembly, metal contamination and natural phosphate concentrations will all interfere with the efficiency of TDAC. Nonetheless, we suggest that this method - as presented here - is robust against many

chromatographically challenging conditions and will facilitate the study of microbial iron cycling, pathogenicity and symbiosis.

CRedit authorship contribution statement

Philipp H. Egbers: Data curation, Conceptualization, Formal analysis, Visualization, Writing - original draft. **Christian Zurhelle:** Formal analysis. **Boris P. Koch:** Writing - review & editing. **Alexandra Dürwald:** Resources. **Tilmann Harder:** Funding acquisition, Supervision, Writing - review & editing. **Jan Tebben:** Funding acquisition, Supervision, Conceptualization, Writing - review & editing.

Declaration of Competing Interest

The authors declare no competing interests.

Data availability

All data provided in the supplementary information will be freely available on the PANGAEA platform upon publication of the manuscript

Acknowledgements

We thank Jennifer Bergemann for support with the bacterial cultures. We thank the late Carl Carrano for the *Marinobacter* strain. We thank Hartmut Becker and Jona Meyer (KRONOS TITAN GmbH.) for the titanium dioxide and the particle size determination. This work was supported by the Deutsche Forschungsgemeinschaft (DFG) in the framework of the priority program “Antarctic Research with comparative investigations in Arctic ice areas” SPP 1158 (TE 1205/3-1, HA 3496/8-1), by the University of Bremen (Exploration Project ZF06A/2019/FB02/Harder_Tilmann) and by the Helmholtz Association (PoF IV ST 6.1, 6.3).

Appendix A. Supplementary data

Supplementary data to this article can be found online at <https://doi.org/10.1016/j.seppur.2022.122639>.

References

- [1] R.C. Hider, X. Kong, Chemistry and biology of siderophores, *Nat. Prod. Rep.* 27 (2010) 637–657.
- [2] M. Hofmann, G. Retamal-Morales, D. Tischler, Metal binding ability of microbial natural metal chelators and potential applications, *Nat. Prod. Rep.* 37 (9) (2020) 1262–1283.
- [3] R.M. Boiteau, D.R. Mende, N.J. Hawco, M.R. McIlvin, J.N. Fitzsimmons, M.A. Saito, P.N. Sedwick, E.F. DeLong, D.J. Repeta, Siderophore-based microbial adaptations to iron scarcity across the eastern Pacific Ocean, *Proc. Natl. Acad. Sci. U. S. A.* 113 (50) (2016) 14237–14242.
- [4] N. Braich, R. Codd, Immobilised metal affinity chromatography for the capture of hydroxamate-containing siderophores and other Fe(III)-binding metabolites directly from bacterial culture supernatants, *Analyst* 133 (2008) 877–880.
- [5] N. Ejje, C.Z. Soe, J.S. Gu, R. Codd, The variable hydroxamic acid siderophore metabolome of the marine actinomycete *Salinispora tropica* CNB-440, *Metallomics* 5 (2013) 1519–1528.
- [6] T. Heine, M. Mehnert, R. Schwabe, D. Tischler, Siderophore Purification via Immobilized Metal Affinity Chromatography, *Solid State Phenom.* 262 (2017) 505–508.
- [7] Y. Li, W. Jiang, R. Gao, Y. Cai, Z. Guan, X. Liao, Fe(III)-based immobilized metal-affinity chromatography (IMAC) method for the separation of the catechol siderophore from *Bacillus tequilensis* CD36, 3, *Biotech* 8 (2018) 392.
- [8] H.G. Upritchard, J. Yang, P.J. Bremer, I.L. Lamont, A.J. McQuillan, Adsorption to metal oxides of the *Pseudomonas aeruginosa* siderophore pyoverdine and implications for bacterial biofilm formation on metals, *Langmuir* 23 (2007) 7189–7195.
- [9] H.G. Upritchard, J. Yang, P.J. Bremer, I.L. Lamont, A.J. McQuillan, Adsorption of Enterobactin to Metal Oxides and the Role of Siderophores in Bacterial Adhesion to Metals, *Langmuir* 27 (2011) 10587–10596.
- [10] J. Xu, P. Wu, E.-C. Ye, B.-F. Yuan, Y.-Q. Feng, Metal oxides in sample pretreatment, *TrAC, Trends Anal. Chem.* 80 (2016) 41–56.
- [11] P.H. Egbers, T. Harder, B.P. Koch, J. Tebben, Siderophore purification with titanium dioxide nanoparticle solid phase extraction, *Analyst* 145 (2020) 7303–7311.
- [12] J. Yang, P.J. Bremer, I.L. Lamont, A.J. McQuillan, Infrared Spectroscopic Studies of Siderophore-Related Hydroxamic Acid Ligands Adsorbed on Titanium Dioxide, *Langmuir* 22 (2006) 10109–10117.
- [13] H. Gulley-Stahl, P.A. Hogan II, W.L. Schmidt, S.J. Wall, A. Buhrlage, H.A. Bullen, Surface Complexation of Catechol to Metal Oxides: An ATR-FTIR, Adsorption, and Dissolution Study, *Environ. Sci. Technol.* 44 (2010) 4116–4121.
- [14] P.Z. Araujo, P.J. Morando, M.A. Blesa, Interaction of Catechol and Gallic Acid with Titanium Dioxide in Aqueous Suspensions. 1. Equilibrium Studies, *Langmuir* 21 (2005) 3470–3474.
- [15] P.A. Connor, K.D. Dobson, A.J. McQuillan, New Sol-Gel Attenuated Total Reflection Infrared Spectroscopic Method for Analysis of Adsorption at Metal Oxide Surfaces in Aqueous Solutions. Chelation of TiO₂, ZrO₂, and Al₂O₃ Surfaces by Catechol, 8-Quinolol, and Acetylacetone, *Langmuir* 11 (1995) 4193–4195.
- [16] L. Petrone, Molecular surface chemistry in marine bioadhesion, *Adv. Colloid Interface Sci.* 195–196 (2013) 1–18.
- [17] A. Tadashi, K.D. Dobson, M.A. James, O. Bunsho, U. Kohei, In Situ Infrared Spectroscopic Studies of Adsorption of Lactic Acid and Related Compounds on the TiO₂ and CdS Semiconductor Photocatalyst Surfaces from Aqueous Solutions, *Chem. Lett.* 27 (1998) 849–850, <https://doi.org/10.1246/cl.1998.849>.
- [18] K. Tani, M. Ozawa, Investigation of chromatographic properties of titania. I. On retention behavior of hydroxyl and other substituent aliphatic carboxylic acids: Comparison with zirconia, *J. Liq. Chromatogr. Relat. Technol.* 22 (6) (1999) 843–856.
- [19] D.H. Green, L.E. Llewellyn, A.P. Negri, S.I. Blackburn, C.J.S. Bolch, Phylogenetic and functional diversity of the cultivable bacterial community associated with the paralytic shellfish poisoning dinoflagellate *Gymnodinium catenatum*, *FEMS Microbiol. Ecol.* 47 (2004) 345–357.
- [20] H.H. Hellmer, M. Holtapps, The Expedition PS124 of the Research Vessel POLARSTERN to the southern Weddell Sea in 2021, in: *Berichte zur Polar- und Meeresforschung = Reports on Polar and Marine Research*, Publisher: Alfred-Wegener-Institut, Helmholtz-Zentrum für Polar- und Meeresforschung, Bremerhaven, Germany, 2021, pp. 1–237, https://doi.org/10.48433/BzPM_0755_2021.
- [21] U. John, G. Rohardt, Continuous thermosalinograph oceanography along Heincke cruise track HE533, in: *PANGAEA* (2019), <https://doi.org/10.1594/PANGAEA.905097>.
- [22] U. John, L. Supraha, S. Gran-Stadniczenko, C. Bunse, A. Cembella, W. Eikrem, J. Janoušková, K. Klemm, N. Kühne, L. Naustvoll, D. Voss, S. Wohlrab, B. Edvardsen, Spatial and biological oceanographic insights into the massive fish-killing bloom of the haptophyte *Chrysochromulina leadbeateri* in northern Norway, *Harmful Algae* 118 (2022), 102287.
- [23] B. Schwyn, J.B. Neilands, Universal chemical assay for the detection and determination of siderophores, *Anal. Biochem.* 160 (1987) 47–56.
- [24] R. Tautenhahn, G.J. Patti, D. Rinehart, G. Siuzdak, X.C.M.S. Online, A Web-Based Platform to Process Untargeted Metabolomic Data, *Anal. Chem.* 84 (2012) 5035–5039.
- [25] P.A. Connor, A.J. McQuillan, Phosphate Adsorption onto TiO₂ from Aqueous Solutions: An In Situ Internal Reflection Infrared Spectroscopic Study, *Langmuir* 15 (1999) 2916–2921.
- [26] V. Rai, N. Fisher, O.W. Duckworth, O. Baars, Extraction and Detection of Structurally Diverse Siderophores in Soil, *Front. Microbiol.* 11 (2020).
- [27] E. Herlinger, R.F. Jameson, W. Linert, Spontaneous autoxidation of dopamine, *J. Chem. Soc., Perkin Trans. 2* (1995) 259–263.
- [28] M.A. Khan, W.T. Wallace, S.Z. Islam, S. Nagpure, J. Strzalka, J.M. Littleton, S. E. Rankin, B.L. Knutson, Adsorption and Recovery of Polyphenolic Flavonoids Using TiO₂-Functionalized Mesoporous Silica Nanoparticles, *ACS Appl. Mater. Interfaces* 9 (37) (2017) 32114–32125.
- [29] J. Kurepa, R. Nakabayashi, T. Paunesku, M. Suzuki, K. Saito, G.E. Woloschak, J. A. Smalle, Direct isolation of flavonoids from plants using ultra-small anatase TiO₂ nanoparticles, *Plant J.* 77 (2014) 443–453.
- [30] W.-J. Liang, Y.-P. Chen, F.-Y. Zheng, S.-X. Li, Titanium dioxide nanoparticle based solid phase extraction of trace Alizarin Violet, followed by its spectrophotometric determination, *Microchim. Acta* 181 (13–14) (2014) 1513–1519.
- [31] J. Yu, W. Wei, M.S. Menyo, A. Masic, J.H. Waite, J.N. Israelachvili, Adhesion of mussel foot protein-3 to TiO₂ surfaces: the effect of pH, *Biomacromolecules* 14 (4) (2013) 1072–1077.
- [32] G. Horányi, Investigation of the specific adsorption of sulfate ions on powdered TiO₂, *J. Colloid Interface Sci.* 261 (2003) 580–583.
- [33] V.E. Kazarinov, V.N. Andreev, A.P. Mayorov, Investigation of the adsorption properties of the TiO₂ electrode by the radioactive tracer method, *J. Electroanal. Chem. Interfacial Electrochem.* 130 (1981) 277–285.